International Journal of Innovative Technology and Exploring Engineering (IJITEE)
ISSN: 2278-3075 (Online), Volume-8 Issue-12, October 2019

Hot Deformation Response of Al 6061-MWCNTs Alloy Composites

D.Jeyasimman, V.Senthilkumar, R.Narayanasamy

Abstract: ***In this investigation, the effect of multi walled carbon nanotubes (MWCNTs) on compressive response with Al 6061 alloy nanocomposites prepared by mechanical alloying has been investigated. Hot deformation tests required to develop processing map were conducted at three temperatures such as 250, 350 and 450°C and in the three strain rates of 0.01, 0.1 and 1.0 s^{-1}. The development of geometric dynamic recrystallization (DRX), dynamic recovery (DRV), instability regions and shear bands were confirmed by characterization study of prepared nanocomposites after hot Compression tests. The average activation energies for hot compression response was calculated as 153.00 KJ/mole for 2 wt.% MWCNTs reinforced Al 6061 alloy (AA 6061) nanocomposites. The most favorable key processing parameters for hot deformation was identified as temperature between 370-450°C and the range of strain rate was 0.1- 0.01s^{-1}. The region which are prone to shear localization, cracks and other instability were identified using the processing map and the same was verified with microstructural images obtained using optical and SEM images.***

Keywords: Constitutive modeling; Flow stress; Hot deformation; Processing map.

I INTRODUCTION

Now a days, aluminum metal matrix composites (AMMCs) are generally preferred in aerospace, defence, automobile sectors because of their specific properties such as light weight, stiffness and high specific strength [1-2]. Strengthening of metal matrix by nano-sized reinforcement particulates attracted many researchers for improving mechanical properties [3]. Amongst the various reinforcements, MWCNTs are increasingly being used due to their distinct properties [4]. Yet, there are various processing routes, Mechanical alloying (MA) is one of the promising route to produce nanometer-sized powder materials and it offer effective, economical and versatile powder metallurgy products [5]. Previous works on mechanical alloying of Al 6061 nonocompsoites reinforced with TiC, Al_2O_3 and MWCNTs nanoparticles have confirmed the formation of nanocrystalline phases [6-8].

Revised Manuscript Received on October 30, 2019.
***** Correspondence Author
D.Jeyasimman*, [a]Department of Mechanical Engineering, Periyar Maniammai Institute of Science and Technology, Vallam, Thanjavur-613403,Tamil Nadu, India.. Email: jeyasimmand@pmu.edu , jeyasimman76@gmail.com
V.Senthilkumar, Department of Production Engineering, National Institute of Technology, Tiruchirappalli-620015, Tamil Nadu, India. Email: guatham07@gmail.com
R.Narayanasamy, Department of Production Engineering, National Institute of Technology, Tiruchirappalli-620015, Tamil Nadu, India. Email: narayan19355@gmail.com

The presence of nanoparticles in the matrix makes a requirement an analysis of hot workability study of nanocomposites. So far, limited works are available about the impact of nanolevel reinforcements on hot compression behavior of non ferrous alloys and nanocomposites synthesized by means of mechanical alloying routes [9-11]. Also the impact of nanolevel material addition to the alloy material on micostructural analysis and workability studies of prepared nanocomposites is prime requirement. Temperature and strain rates are greatly influenced the hot workability properties of prepared nanocomposites. Hence, a detailed investigation of hot workability behavior of multi-walled carbon nanotube reinforced AA 6061 nanocomposites is required.

The uni-axial hot deformation test is performed to give the required data to prepare the constitutive equations [12]. So far, there are various equations which are utilized to describe strain rate, flow stress and temperature relationships. From that, Arrhenius equation and making processing maps through dynamic material model (DMM) is most widely used for characterization of hot deformation behavior.

II EXPERIMENTAL WORK

AA 6061 nanocomposite powders were prepared mixing of various powders (Alfa Aesar, USA) of particle size of 40 µm. Table 1 shows the various powders with its proportions utilized to make AA 6061 nanocomposite. Multi-walled carbon nanotubes (MWCNTs) of 97% purity supplied by Redex Nano Lab, India with 20 nanometer inner diameter, 40 nanometer outer diameter and entire length of 50 µm was used as reinforcement. The all elemental powders were mixed in ball mill apparatus at 280 rpm for 2 h. During the operation of blending, powders only used in the vial. The required process parameters to synthesis of nanocomposites powders through MA, compaction and sintering parameters are shown in Table 2. Due to avoid severe damage of MWCNTs, MWCNTs were added at the last two hours of milling. The preparation of 2 wt.% MWCNTs reinforced AA 6061 nanocomposite powders, nanocomposites and its characterization is explained elsewhere [7].

Table 1. Process Parameters for Mechanical alloying, Composite making.

Mechanical Alloying process parameters	Composite making process parameters
Milling Time: 30 h Bowl and Ball Material: Stainless steel Ball to Powder Ratio: 10:1 (Nine Balls having 20 mm diameter, each weight of 33.5g)	Compaction machine capacity: 40 tons Compact size: Diameter 10 mm and height 13.5 mm Compaction pressure: 500 MPa

Process control agent: Toluene	Lubricant: Zinc Stearate
The plate speed of mill: 100 rpm	Sintering time: 3 h (Reducing atmosphere)
Bowl speed: 280 rpm	Sintering temperature: 723 K, 798 K and 873 K

The hot deformation process parameters on the prepared nanocomposites are shown in Table 2.

Table 2. Hot deformation process parameters

Hot deformation process parameters
Specimens: Cylindrical billet diameter 10 mm and its length 13.5 mm Lubricant: Graphite Hot deformation temperatures: 250, 350 and 450°C Strain rates (SR): 0.01, 0.1 and 1.0 s^{-1}

III RESULTS AND ANALYSIS

3.1 Impact of flow behavior

The true stress–the true strain curves (S-S curves) are drawn for the prepared nanocomposites after testing at various temperatures 250, 350, 450°C under three strain rates such as 0.01, 0.1 and 1.0 s^{-1}. The flow curves for various temperatures were presented in Fig.1.

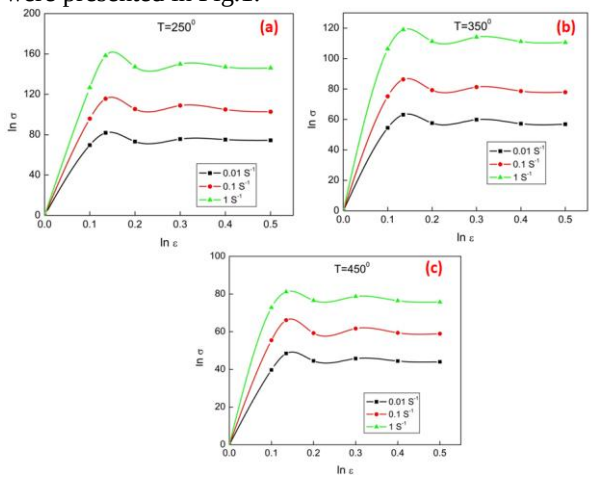

Fig.1. The S-S curves for various temperatures (a) 250°C; (b) 350°C; (c) 450°C.

Initially the S-S curves reach the peak position at a particular stain after that it decrease and maintain steady state up to the final state of hot compression tests. The peak of S-S curves occurs due to high hardening rate and followed steady state occurs due to DRV and DRX in addition to dynamic coarsening (DC) of precipitates during hot compression of light materials and its alloys [11-14]. Strain rate sensitivity (m) was measured by plotting the logarithmic strain in the ordinate and flow stress in abscissa. The m value changes with value of temperatures and strain rates, it will clearly show the difference in slope of the obtained curves. Similar observations were shown in [11-14]. Except for strain rate, all the S-S curves shown a peak flow stress occurs at very nearer to 0.12 strain value, pursue physically by steady state flow softening means constant flow stress that continued until the end [11]. The appearances of the obtained curves have same similarity in all three test conditions. Similar observations were shown in [15- 16]. Initially in the S-S curves stress linearly increases with strain rate due to work hardening (WH) effect and furthermore flow stress is suddenly reduced with strain rate increases due to recovery and recrystallization effect [15]. Finally, WH and Softening effects convert to a steady state balance, so stable flow stress occurs [15]. The impact of the temperatures on S-S curves for particular low strain rate 0.01 was observed and shown in Fig. 2.

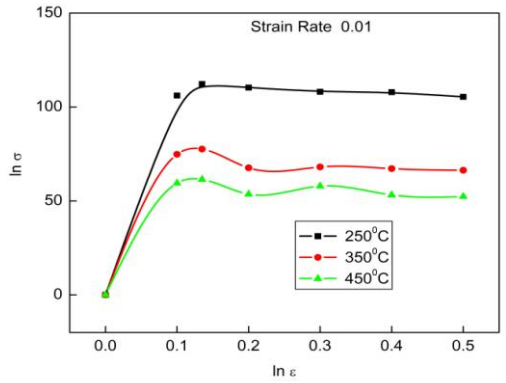

Fig.2. The impact of the temperatures on S-S curves for particular low strain rate 0.01.

Hot compression test gives the value of force and displacement. Using the force and displacement value, the true strain and true stress value are calculated.

The inter-relationship between flow stress (σ), strain rate (ε), the apparent activation energy (Q), temperature (T) Zener–Hollomon parameter (Z) and material constants n, A1 and A2 making during hot compression tests of nanocomposites can be evaluated based on previous study by Ahamed et al. [11];

$$\sigma = P(1-e)\times a \quad (1)$$

$$\varepsilon = \ln(1-e) \quad (2)$$

$$\varepsilon = A\times\left(\sinh(\alpha\sigma)\right)^{n}\times e^{-Q/RT} \quad (3)$$

$$\varepsilon = A1(\sigma)^{n1} \quad (4)$$

$$\varepsilon = A2(e^{\beta\sigma}) \quad (5)$$

$$\ln(\varepsilon) = \ln A1 + n\ln\sigma \quad (6)$$

$$\ln(\varepsilon) = \ln A2 + \beta\sigma \quad (7)$$

$$\alpha = \frac{\beta}{n1} \quad (8)$$

Zener Holloman parameter (Z) proposed by Yonghua Duan et al. [16] and the activation energy proposed by Yandong Jia et al. [17];

$$Z = A\times(Sinh\alpha\sigma)^{n} \quad (9)$$

$$Q = -R \times \left(\frac{d(\ln \varepsilon)}{d(\ln \sinh(\alpha\sigma))} \right) \times \left(\frac{d(\ln \sinh(\alpha\sigma))}{\left(\frac{d}{T}\right)} \right) \quad (10)$$

The apparent activation energy Q value may be calculated from the slope values obtained from the above plots [11];

$$\ln Z = \ln A + \ln \sinh(\alpha\sigma) \quad (11)$$

Replacing the values for A, α, n and Q in Equation (3), a hot compression constitutive equation may be developed and is used to calculate the flow stress for the prepared nanocomposites.

The ln (Z) value for various temperatures and strain rate states are shown in Table 4.

Table 4. Zener Holloman parameter (Z) values under various input conditions.

Temperatures, K	Zener Holloman Values for various strain rates (SR), s^{-1}		
	0.01	0.1	1.0
523	39.87	40.16	40.36
623	36.31	36.77	37.12
723	33.50	33.90	34.20

From this Table, Z value is linearly increased with improvement in strain rates can be noticed. For temperature 523 K, Z values are high because of work hardening (WH) is high at this temperature and also the Zener Holloman (Z) value are reduces with temperature increases caused by softening mechanisms [18].

Estimated flow stress values calculated by the Equation (9)

$$\sigma = \frac{1}{n} \left(Sinh^{-1} \left(\frac{\varepsilon e^{\frac{Q}{RT}}}{A} \right)^{\frac{1}{n}} \right) \quad (12)$$

The relationship between various parameters such as σ, ε, ln (Z) and T^{-1} for 0.5 strain rate of AA 6061-2 wt.% MWCNTs nanocomposites are shown in Figs.3 (a)-(d). The above relationship gives the resolution of different parameters like as n, A and α [19-20].

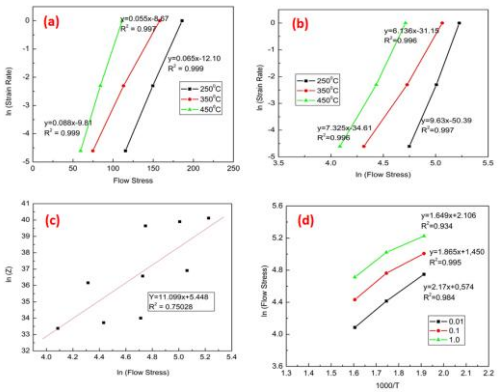

Figs. 3. The various relationship of AA 6061-2 wt.% MWCNTs nanocomposites for 0.5 SR (a) Flow stress (σ) and Strain rate (ε) ; (b) ln (σ) and ln (ε); (c) ln (σ) and ln (Z); (d) ln (σ) and T^{-1}

Figs. 4(a)-(b) shows the correlation among the two variables such as flow stress (FS) and strain rate (SR) for AA 6061-2 wt.% MWCNTs nanocomposites for SR 0.1 s^{-1} and 0.5 s^{-1}.

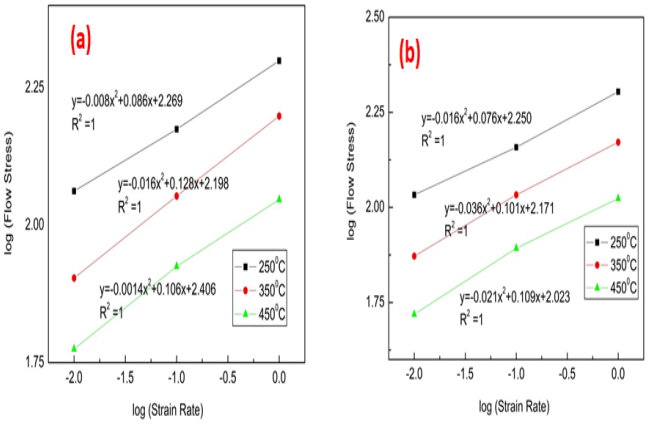

Figs. 4. The correlation among Log (σ) and Log (ε) of AA 6061-2 wt.% MWCNTs nanocomposites (a) for 0.1 SR; (b) for 0.5 SR

The relationship between various parameters such as ln(Sinh(ασ)), ln (ε), ln (Z) and T^{-1} for 0.1 strain rate of AA 6061-2 wt. MWCNTs nanocomposites are shown in Figs.5 (a)-(c).

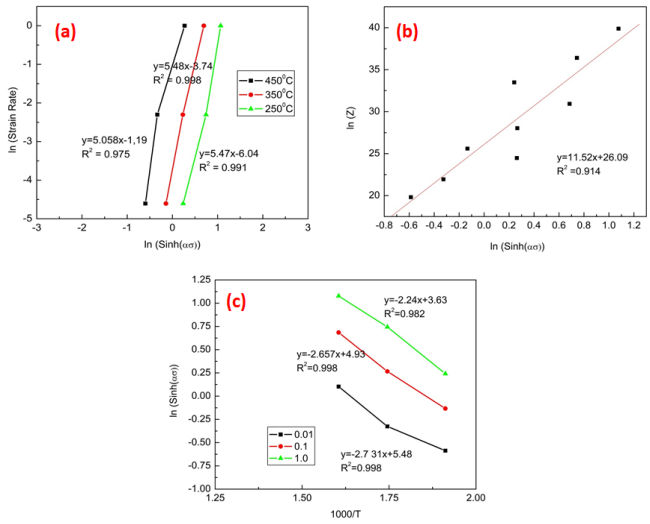

Figs.5. The various relationship of AA 6061-2 wt.% MWCNTs nanocomposites for 0.1 SR (a) ln (Sinh(ασ)) and ln (ε); (b) ln (Sinh(ασ)) and ln (Z); (c) ln (Sinh(ασ)) and T^{-1}

The inter-relationship among various parameters such as ln (Sinh(ασ)), ln (ε), ln (Z) and T^{-1} for 0.5 strain rate of AA 6061-2 wt.% MWCNTs nanocomposites are shown in Figs.6 (a)-(c). The slope value gives stress exponent value n and it is obtained in the range between 4.93 to 5.61.

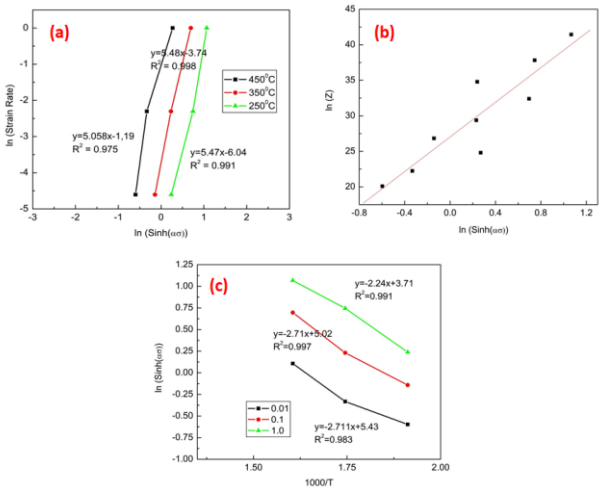

Figs.6. The various relationship of AA 6061-2 wt.% MWCNTs nanocomposites for 0.5 SR (a) ln (Sinh(ασ)) and ln (ε); (b) ln (Sinh(ασ)) and ln (Z); (c) ln (Sinh(ασ)) and T^{-1}

The contrast of the estimated and experimental FS of AA 6061-2 wt.% MWCNTs nanocomposites after hot deformation for relative strain 0.1 and relative strain 0.5 are shown in Figs.7(a)-(b).

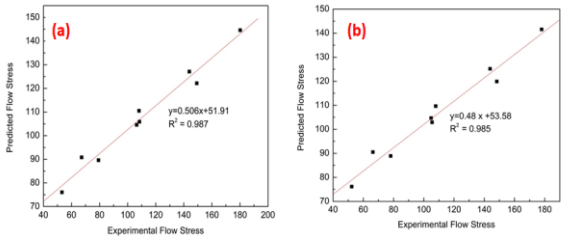

Figs.7. The contrast of estimated and experimental FS of AA 6061-2 wt. % MWCNTs nanocomposites (a) for relative strain 0.1; (b) for relative strain 0.5.

3.2. Processing Map

Processing maps are drawn after the hot deformation test depends on Dynamic Materials Model (DMM). The following expressions gives the determination of various hot deformation parameters such as stress (σ), power (p) extracted respectively prepared nanocomposites, strain rate sensitivity (m), dimensionless parameter (η), maximum possible dissipation J_{max} and the instability parameter (ξ(ε)). This was explained elsewhere [11].

$$\sigma = k\left(\varepsilon^{m}\right) \tag{13}$$

$$p = \sigma \times \varepsilon \tag{14}$$

$$p = \sigma\varepsilon = \int_0^{\sigma} \varepsilon d\sigma + \int_0^{\varepsilon} \sigma(d\varepsilon) = J + G \tag{15}$$

$$m = \frac{dJ}{dG} = \frac{\varepsilon d\sigma}{\sigma d\varepsilon} \cong \frac{d\log\sigma}{d\log\varepsilon} \tag{16}$$

$$J = J_{\max} = \frac{\sigma\varepsilon}{2} \tag{17}$$

$$\eta = \frac{J}{J_{\max}} = \frac{2m}{m+1} \tag{18}$$

$$\xi(\varepsilon) = \left(\frac{d\ln\left(\frac{m}{m+1}\right)}{d\varepsilon} \right) + m \le 0 \tag{19}$$

The instability map was drawn based on the above equation proposed by Bin-Jian LV et al. [21] and various flow instabilities region was marked at temperature and strain rate space.

3.3 Constitutive Model and Verification of Model

Arrhenius constitutive model is used for constitutive modeling because it gives good correlation between strain rate and temperature. Activation energy and material constant calculated for different strain value and constitutive model proposed for given nanocomposite material. The apparent activation energy Q, flow stress α, materials constants A and n values for various strain levels for Arrhenius hyperbolic model were shown in Table 5.

Average activation energy comes 153.00 kJ/mole which is more than activation energy of pure aluminum alloy value which is 142 kJ/mole. Average value of n is 7.282. The higher Q value is because of improved resistance for dislocations movement particularly in the nanocomposites caused by the nanoparticle pinning. Using proposed constitutive equations predicted flow stress values calculated. These values are accurately correlated with experimental value with R value 0.998, which shown that the given model is correct. Scanning electron microscope (SEM) images of hot deformed nanocomposites at 0.1 strain rate with varying temperatures are shown in Figs.8(a)-(c).

Table 5. The apparent activation energy Q, flow stress α, materials constants A and n values for various strain levels of AA 6061-2wt. % MWCNTs Nanocomposites

Strain	Q/(KJ-Mol^{-1})	α/MPa^{-1}	A	n
0.1	151.72	0.0093	1.89 X 10^{13}	7.697
0.2	140.62	0.0096	1.92 X 10^{13}	7.071
0.3	147.69	0.0097	1.90 X 10^{13}	7.468
0.4	148.13	0.0099	1.98 X10^{13}	7.086
0.5	153.00	0.0101	2.01 X10^{13}	7.087

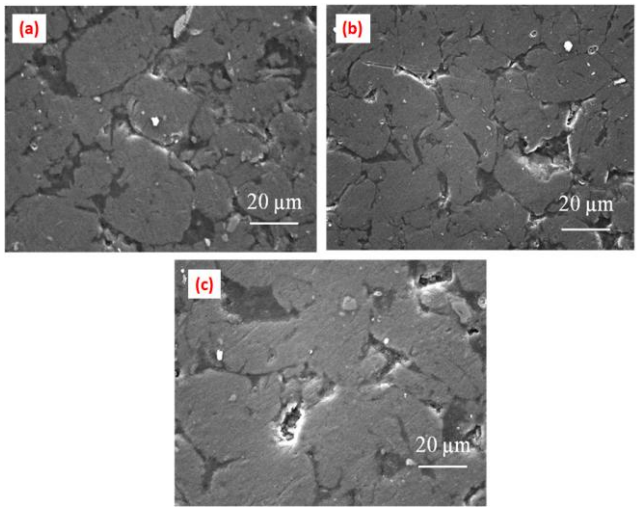

Figs. 8. SEM images of hot deformed AA 6061-2 wt. % MWCNTs nanocomposites at 0.1 strain rate at (a) 250^{0}C; (b) at 350^{0}C; (c) at 450^{0}C.

Process maps are drawn for different strain 0.4 and 0.5 and instability region also shown in the Figs. 9(a)-(b). The instability region occurs at high strain rate, as the strain increases the instability region also increased. There may be much reason for instability such as adiabatic shear band, cracks grain boundary sliding etc. This was supported by earlier studies [15, 22-23]. Fig.10 shows the shear band localization in the prepared nanocomposites after deformation test.

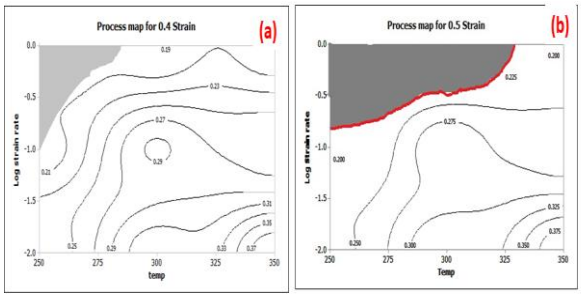

Figs.9. Processing maps for (a) 0.4 SR; (b) 0.5 SR

Instability region initial start at high SR with very low temperature and is propagated up to high SR with high temperature as strain value increases. The highest efficiency for strain 0.4 and 0.5 is, 35%, 43% respectively. The higher efficiency region comes at higher temperature and lower SR. This result was confirmed by previous studies results [31-33].

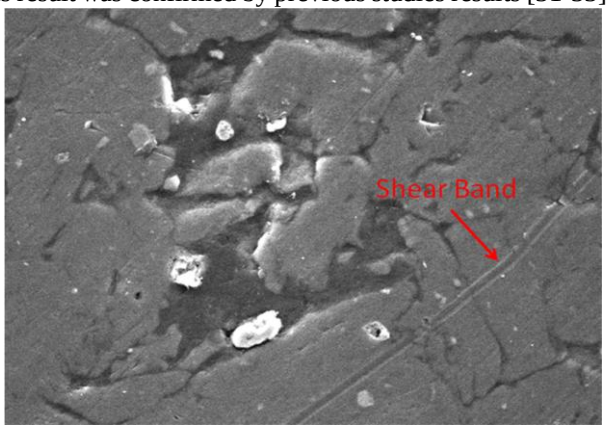

Fig.10. Shear band occurs in AA 6061-2 wt. % MWCNTs nanocomposite

IV CONCLUSION

Flow stress (FS) value differs with change in SR and temperature values. The given Arrhenius constitutive model describes the flow behavior of the prepared nanocomposites for the combination of given temperature and SR. Process maps drawn and the workability region occur at the combination of temperature and SR. The maximum efficiency is 43.21% at strain 0.5 which occur at 450° and 0.01 SR. The optimum region for hot compression test is in the temperature range 370-450° and SR between 0.1- 0.01 s^{-1}. The safe working zone is identified for various combinations of SR and temperature which are necessary for any material to make it useful product. The region which are prone to shear localization, cracks and other instability were identified using the processing map and the same was verified with microstructural images obtained using optical and SEM images.

REFERENCES

1. S.Tahamtan, A.Halvaee, M.Emamy and M.S. Zabihi, Fabrication of Al/A206-Al2O3 nano/micro composite by combining ball milling and stir casting technology. *Mater. Des., 2013,* **49,** p 347-359.
2. S.M.Zebarjad and S.A.Sajjadi, Dependency of physical and mechanical properties of mechanically alloyed Al-Al_2O_3 composite on milling time. *Mater. Des.*, 2007, **28,** p 2113-2120.
3. H.R.Ezatpour, S.A.Sajjadi, A.Chaichi and G.R.Ebrahimi, Mechanical and microstructure properties of deformed Al-Al2O3 nanocomposite at elevated temperature. *J. Mater. Research,* 2017, **32** (6), p 1118-1128.
4. R.George, K.T.Kashyap, R.Rahul and S.Yamadagini, Strengthening in carbon nanotube/aluminum (CNT/Al) composites. *Scripta Mater.*, 2005, **5,** p 1159-1163
5. C.Suryanarayana, Mechanical alloying and milling. *Prog. Mater. Sci.*, 2001, **46** p 1-184.
6. D.Jeyasimman, S.Sivasankaran, K.Sivaprasad, R.Narayanasamy and R.S.Kambali, An investigation of synthesis, consolidation and mechanical behaviour of Al 6061 nanocomposites reinforced by TiC via mechanical alloying. *Mater. Des., 2014,* **7,** p 394-404.
7. D.Jeyasimman, K.Sivaprasad, S.Sivasankaran and R.Narayanasamy. Fabrication and consolidation behavior of Al 6061 nanocomposite powders reinforced by multi-walled carbon nanotubes. *Powder Technol.*, 2014, **258**, p 189-197.
8. D.Jeyasimman, K.Sivaprasd, S.Sivasankaran, R.Ponalugusamy, R.Narayanasamy and Vijay Kumar Iyer. Microstructural observation, consolidation and mechanical behaviour of AA 6061 nanocomposites reinforced by γ-Al_2O_3 nanoparticles. *Adv. Powder. Technol*., 2015, **26**, p 139-148.
9. V.Senthilkumar, A.Balaji and R. Narayanasamy, Analysis of hot deformation behavior of Al 5083–TiC nanocomposite using constitutive and dynamic material models. *Mater. Des., 2012,* **37,** p 102–110.
10. L. Shi, H. Yang, L.G. Guo and J. Zhang, Constitutive modeling of deformation in high temperature of a forging 6005A aluminum alloy. *Mater. Des., 2014,* **54,** p 576–581
11. Hafeez Ahamed and V. Senthilkumar, Hot deformation behavior of mechanically alloyed Al6063/0.75Al2O3/0.75Y2O3 nanocomposite—A study using constitutive modeling and processing map. *Mater. Sci. and Eng. A, 2012,* **539**, p 349–359
12. M.R.Rokni, A Zarei-Hanzaki, Ali A Rosstaei and A.Abolhasani, Constitutive base analysis of 7075 aluminium alloy during hot compression testing. *Mater. Des.*, 2012 **32**(10), p 4955-4960
13. M. Rajamuthamilselvan and S. Ramanathan, Hot deformation behaviour of 7075 alloy, *J. Alloys Compd.*, 2011, **509**, p 948–952.
14. Zhang Peng, Chao Hua, Chao-gang Ding, Qiang Zhu and He-yong Qin, Plastic deformation behavior and processing maps of a Ni-based super alloy *Mater. Des., 2015,* **65**, p 575–584

15. Hafeez Ahamed and V. Senthilkumar, Prediction of flow stress during hot deformation of MA'ed hybrid aluminium nanocomposite employing artificial neural network and Arrhenius constitutive model. *Multidiscipline Modeling in Mater. and Struct.* 2012, **8**(2), p 136-158.
16. Yonghua Duan, Lishi Ma, Huarung Qi, Runyue Li, Ping Li, Developed constitutive models, processing maps and microstructural evolution of Pb-Mg-10Al-0.5B alloy. *Mater. Character.*, 2017, 129, p 353-66.
17. Yandong Jia, Fuyang Cao, Shu Gueo, Pan Ma, Jingshun Liu, Jianfei Sun, Hot deformation behavior of Spray-deposited Al-Zn-Mg-Cu alloy. *Mater. Des., 2014,* **53,** p 79-85.
18. L Saravanan and T.Senthilvelan, Investigations on the hot workability characteristics and deformation mechanisms of aluminuim alloy-Al_2O_3 nanocomposites. *Mater. Des., 2015,* **79**, p 6-14.
19. J. Porntadawit, V. Uthaisangsuk and P. Choungthong, Modeling of flow behavior of Ti–6Al–4V alloy at elevated temperatures, *Mater. Sci. and Eng. A 2014,* **599**, p 212-222.
20. R.S.Sundar, D.H. Sastry and Y.V.R.K. Prasad, Hot workability of as-cast Fe3Al_ 2.5% Cr intermetallic alloy, *Mater. Sci. and Eng. A, 2013,* ***347,*** p 86-92.
21. Bin-Jiang LV, Jian Peng, Li-Li Zhu, Yong-Jian Wang, Ai-Tao Tang. The effect of 14 H LPSO phase on dynamic recrystallization behavior and hot workability of Mg-2.0 Zn-0.3Zr-5.8Y alloy. *Mater Sci Eng A,* 2014, **599,** p 150-59.
22. H.Zhang, J.Li, D.Yuan and D.Peng, Hot Deformation behavior of new Al-Mg-Si-Cu aluminium alloy during compression at elevated temperatures, *Mater. Charact.*, 2007, **58**, p 168-173.
23. Nangping Jin, Hui Zhang, Yi Han, Wenxiang Wu and Jianghua Chen, Hot deformation behavior of 7150 aluminum alloy during compression at elevated temperature, *Mater. Charact.*, 2009, **60**, p 530-536.

AUTHORS PROFILE

First Author- Dr. D. Jeyasimman working as a Associate Professor and Head of Department in the Department of Mechanical Engineering, Periyar Maniammai Institute of Science & Technology, Thanjavur, Tamil Nadu, India. He has completed his Full Time Ph.D. research work in nanocomposites area. He has more than 20 good publications in international journals (with high impact factors) and thirteen years teaching experience in various engineering colleges & Universities. He has obtained his postgraduate degree in Manufacturing Engineering in Anna University, Chennai, India. He has obtained his undergraduate degree in Mechanical Engineering in Bharathiyar University, Coimbatore, Tamil Nadu, India.

Second Author Dr.V.Senthilkumar is Associate Professor of Department of Production Engineering at NIT, Tiruchirappalli with over 20 years of teaching and research experience. He has published more than 50 papers in International Journals and made 20 International conference presentations. He completed many research based projects and consultancy works getting funds from various agencies such as DST, CSIR and BHEL. His areas of specializations are Manufacturing Process Modelling, process design, Advanced Materials Processing and Powder Metallurgy.

Third Author Dr.R.Narayanasamy is Professor of Department of Production Engineering at NIT, Tiruchirappalli with over 40 years of teaching and research experience. He has published more than 200 papers in International Journals and made 40 International conference presentations. He completed many research based projects and consultancy works getting funds from various agencies. His areas of specializations are Metal Forming and Powder Metallurgy.